Dynamics of synaptically coupled integrate-and-fire-or-burst neurons

S Coombes[*]

Department of Mathematical Sciences,

Loughborough University, Leicestershire, LE11 3TU, UK.

(Dated: February 3, 2003)

Abstract

The minimal integrate-and-fire-or-burst (IFB) neuron model reproduces the salient features of experimentally observed thalamocortical (TC) relay neuron response properties, including the temporal tuning of both tonic spiking (i.e., conventional action potentials) and post-inhibitory rebound bursting mediated by a low-threshold calcium current. In this paper we consider networks of IFB neurons with slow synaptic interactions and show how the dynamics may be described with a smooth firing rate model. When the firing rate of the IFB model is dominated by a refractory process the equations of motion simplify and may be solved exactly. Numerical simulations are used to show that a pair of reciprocally interacting inhibitory spiking IFB TC neurons supports an alternating rhythm of the type predicted from the firing rate theory. A change in a single parameter of the IFB neuron allows it to fire a burst of spikes in response to a depolarizing signal, so that it mimics the behavior of a reticular (RE) cell. Within a continuum model we show that a network of RE cells with on-center excitation can support a fast traveling pulse. In contrast a network of inhibitory TC cells is found to support a slowly propagating lurching pulse.

---

[*]Electronic address: s.coombes@lboro.ac.uk; URL: `http://www.lboro.ac.uk/departments/ma/staff/coombes/`

I.   INTRODUCTION

Rhythmic bursting is a hallmark feature of mammalian thalamocortical networks during slow wave sleep, attentiveness, and generalized seizures. One of the most studied collective oscillations is that of spindling which occurs spontaneously at the onset of sleep or drowsiness (see e.g., [1]). Spindle waves propagate to the cerebral cortex from the thalamus where they are recorded in the electroencephalogram as a 7-14 Hz oscillation. They are currently believed to be generated through a cyclical interaction between populations of thalamocortical and thalamic reticular or perigeniculate neurons involving both the intrinsic membrane properties of these neurons and their anatomical interconnections. For example, spindle like waves have been observed in ferret brain splice preparations which preserve anatomical interactions between perigeniculate (PGN) and dorsal lateral geniculate nucleus (LGNd) thalamocortical neurons and travel with a speed of around 1mm/s [2, 3, 4, 5]. These waves are produced as a sequence of inhibition in thalamocortical cells followed by rebound bursts of action potentials. Burst firing in relay neurons then excites PGN neurons, thereby completing the loop and starting the next cycle of oscillation. Simultaneously, PGN neurons regulate each others firing through lateral inhibitory interactions. Reticular (RE) thalamic and thalamocortical (TC) neurons both possess a so-called slow T-type calcium current that allows them to generate either rhythmic burst or tonic firing patterns. This current is associated with an influx of calcium ions and leads to a large membrane depolarization on which more conventional spikes generated by other fast currents may ride, resulting in a burst response. Typically RE cells respond with a burst of action potentials in response to a brief depolarization, whilst TC cells respond via post-inhibitory rebound. In this mode the cell must be hyperpolarized and then released from inhibition before it can fire a burst. A number of computational models have been developed that incorporate both the intrinsic membrane properties of RE and TC cells and their anatomical interconnections. The work of Destexhe *et al.* (see e.g., [6]) was developed based on electrophysiological measurements in ferret thalamic slices and reproduces successfully the characteristics of spindle oscillations observed in vitro. Importantly, local axonal arborization of the TC to RE and RE to TC projections allows oscillations to propagate through a network. The model of Golomb *et al.* [7] also uses single compartment models with detailed models of relevant ionic currents to reproduce many of the experimental results from in vitro ferret thalamic slice preparations.

Moreover, this work highlights the possibility of waves which may advance in a lurching manner. Simplifications of such circuits by Rinzel *et al.* [8] in which RE cells are endowed with the rebound property has allowed a reduction to a single layered network that still supports propagating waves. They make the observation that if the synaptic connectivity is on-centered then lurching propagation occurs, but that smoothly propagating waves can be found when the connectivity is off-centered. Although biophysically realistic such models are typically hard to analyze. The difference between smooth and lurching waves has been explored analytically within a simpler integrate-and-fire network with conduction delays by Golomb and Ermentrout [9, 10]. They show that as a discrete communication delay between neurons increases a smoothly propagating pulse can lose stability in favor of a lurching wave. Short conductance delays are considered to mimic the off-centered networks considered by Rinzel *et al.* which essentially allow the cells to escape from inhibition sufficiently quickly so as to favor smooth propagation. The full network equations of Rinzel *et al.* have recently been studied by Terman *et al.* [11] using techniques from geometric singular perturbation theory. They derive explicit formulas for when smooth and lurching waves exist and also determine the effect of network parameters on wave speed. This work relies partly on numerically determined properties of the single cell model. In this paper we return to some of the issues raised by these computational and analytical studies of thalamic networks. By working with a recently introduced minimal model of a spiking cell possessing a slow T-type calcium current we show that it is possible to analyze rhythmic bursting and the smooth and lurching propagation of waves exactly. Our results are entirely consistent with earlier work, and open up the way for further studies of thalamocortical networks from a mathematical perspective. In section II we describe the basic neuron model that we work with. This is the integrate-and-fire-or-burst (IFB) model recently shown by Smith *et al.* [12] to be able to reproduce many of the salient features of experimentally observed thalamocortical relay neuron response. This includes the temporal tuning of both tonic spiking (conventional action potentials) and post-inhibitory rebound bursting mediated by a low threshold calcium current. As it stands this model can fire arbitrarily fast, which is somewhat at odds with the well known refractory property of real neurons. To remedy this we adopt an approach often used with the simpler integrate-and-fire neuron model and introduce an appropriate time-dependent threshold. For slowly varying time dependent input signals we derive a firing rate approximation of this IFB model. Moreover, when the firing rate is dominated by a

refractory process (such as the one introduced) we show how to exactly construct solutions which are frequency locked to that of a periodic stimulus. This approach is extended in section III to cover synaptically interacting networks of IFB neurons. As an example of the power of the firing rate formalism we exactly solve the dynamics for a simple central pattern generating circuit of half-center type. A comparison with numerical simulations of the spiking model shows a good quantitative agreement for slow synapses. In section IV we consider a two-layer network of interacting TC and RE cells in two different extremes. In the first case we consider a one-dimensional network of RE cells interacting through an indirect excitatory path. In the second case we consider the opposite scenario in which TC cells interact indirectly via an inhibitory path. For the excitatory RE network we are able to construct a smooth traveling pulse, with speeds in agreement with direct numerical simulations. These same simulations show that of the two possible branches of traveling pulse solutions it is the faster that is stable. The inhibitory TC network on the other hand naturally supports lurching pulses. Again we show excellent agreement between theory and numerical experiment, but this time it is the slower of the two possible lurching waves that is stable. Finally in section V we discuss extensions of our work to more realistic networks and consider how the framework we have presented is useful for addressing issues relating to sensory processing in thalamic networks.

II.   THE MODEL AND ITS REDUCTION

All thalamic relay cells respond to excitatory inputs in one of two different modes, which are known as burst and tonic. The response mode depends on the state of a voltage- (and time-) dependent inward Ca^{2+} current that is known as I_T, because it involves T-type Ca^{2+} channels located in the membranes of the soma and dendrite. In burst mode, I_T is activated and an inflow of Ca^{2+} produces a depolarizing waveform, known as the low threshold spike (LTS) that, in turn, usually activates a burst of conventional action potentials. When a relay cell has been relatively depolarized for ~ 100 ms or more, I_T becomes inactivated and the cell fires in tonic mode. However, after ~ 100ms or more of relative hyperpolarization, inactivation of I_T is alleviated and the cell fires in burst mode. A minimal model of this process has been developed by Smith *et al.* and is described in [12]. In essence this model may be regarded as an integrate-and-fire (IF) model with the addition of a slow variable.

4

The dynamics of this slow variable underlies the generation of bursts and motivates the name integrate-and-fire-or-burst (IFB). In more detail the current balance equation for the IFB model is

$$C\frac{\mathrm{d}v}{\mathrm{d}t} = -I_L - I_T - I, \tag{1}$$

where C is a membrane capacitance, v the membrane voltage, I represents a synaptic current and $I_L = g_L(v - v_L)$ is a leakage current with constant conductance g_L and leakage reversal potential v_L. The low-threshold Ca^{2+} current is given by $I_T(t) = g_T h(t)(v - v_T)\Theta(v - v_h)$ where $\Theta(\cdot)$ is a Heaviside step function and the slow variable h has dynamics:

$$\tau_h(v)\frac{\mathrm{d}h}{\mathrm{d}t} = -h + h_\infty(v), \tag{2}$$

and $h_\infty(v) = \Theta(v_h - v)$ with $\tau_h(v) = \tau_h^- \Theta(v - v_h) + \tau_h^+ \Theta(v_h - v)$. Equation (2) incorporates the de-inactivation of the low-threshold Ca^{2+} conductance, which involves T-type Ca^{2+} channels and produces the transmembrane current, I_T. The de-inactivation level of I_T relaxes to zero with time constant τ_h^- when $v \geq v_h$ and relaxes to unity with time constant τ_h^+ when $v < v_h$. Hence, sufficient hyperpolarization leads to increasing values of h, representing de-inactivation of I_T. An action potential is said to occur whenever the membrane potential v reaches some threshold v_θ. The set of action potential firing times are defined by

$$\sigma_n = \inf\{t \mid v(t) \geq \gamma \ ; \ t \geq \sigma_{n-1}\}, \tag{3}$$

for some voltage threshold γ. Immediately after a firing event the system undergoes a discontinuous reset such that $v(\sigma_n^+) = v_{\mathrm{reset}}$. Hence, the flow generated by the IF process is discontinuous at the firing times $t = \sigma_n$. As it stands the standard IF mechanism does not allow for the possibility of a refractory process. One way to incorporate this within the IF framework is to allow the threshold function to be time dependent. Large threshold increases just after a firing event, and subsequent decay back towards a constant threshold value at a rate τ_R, can ensure that spikes times are more consistent with those of real neurons. Here τ_R is identified as the refractory time scale of the model neuron. We write this refractory process in the form

$$\tau_R\frac{\mathrm{d}\gamma}{\mathrm{d}t} = -\gamma + v_\theta, \qquad \gamma(\sigma_n^+) = \gamma(\sigma_n) + \gamma_0, \tag{4}$$

for some large positive constant γ_0. Throughout this paper we shall take $\tau_R = 5\mathrm{ms}$ and $\gamma_0 = 100\mathrm{mV}$. The remaining standard parameters of the IFB model (obtained from fits with experimental data) are given in Table 1.

Parameter	Value	Unit
v_θ	-35	mV
v_L	-65	mV
C	2	μF/cm^2
g_L	0.035	mS/cm^2
v_{reset}	-50	mV
v_h (TC)	-70	mv
v_h (RE)	-60	mv
v_T	120	mv
τ_h^-	20	ms
τ_h^+	100	ms
g_T	0.07	mS/cm^2

TABLE I: Standard cellular parameters for the IFB model, obtained from fits with experimental data [12].

One of the striking abilities of the IFB neuron model is its ability to mimic the behavior of both thalamocortical (TC) and reticular (RE) cells. For TC cells we take $v_L > v_h$, and for RE cells it is more appropriate to choose $v_L < v_h$ [13]. With these choices an IFB RE cell can fire a burst in response to a depolarizing signal, whilst an IFB TC cell can operate in rebound mode (as described in section I). The IFB dynamics depends strongly on the two thresholds v_h and v_θ, responsible for the activation of burst and tonic spiking, respectively. Indeed, by exploiting the linearity of the model between these thresholds it has been possible to give a complete account of mode-locked solutions that arise in response to periodic forcing [14]. This *exact* approach requires the simultaneous solution of a set of nonlinear algebraic equations to keep track of firing times (one for each spike). Hence, it is cumbersome when dealing with rhythms in which one wishes to keep track of a large numbers of spikes riding an LTS. This encourages the search for reduced descriptions which require less attention to the precise timing of spikes. If the dynamics for $h(t)$ and the synaptic drive $I(t)$ is *slow* compared to that of $v(t)$, then it is natural to look for a firing rate model that can capture the full spiking dynamics in a semi-quantitative manner [15]. For later convenience we write the synaptic input in the form $I(t) = u(t)(v - v_u)$. The sign of v_u relative to the resting

potential determines whether a synapse is excitatory or inhibitory. To derive a firing rate model we imagine that a steady state value of v exists that may be parameterized by h and u as the solution to

$$v(h, u) = \frac{g_L v_L + g_T v_T h \Theta(v(h, u) - v_h) + v_u u}{g_L + g_T h \Theta(v(h, u) - v_h) + u}. \tag{5}$$

Note that there are two possible solutions of (5). We take the instantaneous firing rate of the IFB neuron to be $f(v(h, u))$, where

$$f(v) = \left\{ \tau_R + \tau \ln \left[\frac{v - v_{\text{reset}}}{v - v_\theta} \right] \right\}^{-1} \Theta(v - v_\theta), \qquad \tau = \frac{C}{g_L}. \tag{6}$$

This is recognised as the standard firing rate response of a refractory IF neuron to constant forcing (see for example [16]). Here we assume that the refractory mechanism limits the rate to at most τ_R^{-1}, and that to a first approximation the IF neuron fires when $v = v_\theta$. In the original IFB model, a burst of action potentials is expected whenever the membrane potential, v, crosses the burst threshold v_h from below. From a dynamical systems viewpoint it is natural to adopt a description of the firing rate model where

$$v(h, u) = \frac{g_L v_L + g_T v_T h s + v_u u}{g_L + g_T h s + u}, \tag{7}$$

and $s \in \{0, 1\}$ is set to 1 if $v(h, u)$ crosses v_h from below and s is set to 0 if v crosses v_h from above. This provides a consistent mechanism for choosing between possible coexisting solutions of (5). The full spiking model is expected to be well approximated by the rate model in the formal limit $C \to 0$.

To illustrate the usefulness of such a reduction we compare the behavior of the original and reduced model to an oscillatory stimulus of the form $u(t) = I(1 + \cos(\omega t))$. An example of a spiking IFB waveform that results from such a drive is shown in Fig. 1. The signal $u(t)$ has a phase shift ϕ, with respect to some resultant Δ-periodic orbit $v(t) = v(t + \Delta)$. This means that we may write $v(t) = v(h(t), u(t - \phi\Delta))$ for $t \in [0, \Delta)$. For simplicity we shall focus on the case that $\Delta = 2\pi/\omega$ (i.e., a 1:1 frequency locked state). It is a simple matter to exploit the piecewise linear nature of the rebound dynamics to calculate that

$$h(t) = \begin{cases} \overline{h} e^{-t/\tau_h^-} & 0 \leq t \leq \Delta^+ \\ \overline{h} e^{-\Delta^+/\tau_h^-} e^{-(t-\Delta^+)/\tau_h^+} + 1 - e^{-(t-\Delta^+)/\tau_h^+} & \Delta^+ < t < \Delta \end{cases}, \tag{8}$$
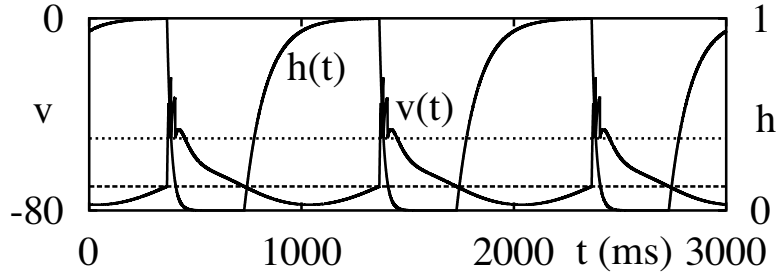
FIG. 1: An illustration of IFB output under periodic sinusoidal inhibitory stimulation. $I = 0.01$, $\omega = 2\pi$, $v_h = -70$ and $v_u = -100$.

for some $\Delta_+ < \Delta$. The function $h(t)$ is periodically extended outside its principal domain. The value of $\overline{h} \equiv h(0)$ is given by

$$\overline{h}(\Delta_+, \Delta) = \frac{1 - e^{-(\Delta - \Delta^+)/\tau_h^+}}{1 - e^{-\Delta^+/\tau_h^-} e^{-(\Delta - \Delta^+)/\tau_h^+}}. \tag{9}$$

The two unknowns Δ^+ and ϕ may be found by the simultaneous solution of the two equations $v(\Delta^+) = v_h$ and $v(\Delta) = v_h$. The numerical solution of this system of equations may be used to calculate regions in parameter space where periodic solutions exist. In Fig. 2 we show the phase space trajectory of a periodic orbit for both the IFB spiking and rate models. The spiking orbit is calculated numerically, whilst the orbit in the rate model is obtained in closed form. The orbit of the rate model provides an *envelope* for the spiking dynamics. Although it cannot track voltage spikes, it does accurately capture the duration of bursting (by causing a high firing rate) as well as tracking the non-spiking part of the orbit very well. With more work it is also possible to obtain the spiking orbit in closed form, but we shall not pursue this here. A detailed study of the full spiking model for such a periodic drive can be found in [14]. Importantly it is very easy to obtain quantities such as Δ^+, within the firing rate framework, as a function of system parameters without recourse to direct numerical simulations. For example using this approach Δ^+ is predicted to be a monotonically decreasing function of the stimulus frequency. An examination of Δ^+ for the spiking model shows that this trend is respected with increasing agreement between rate and spike models as C is decreased (not shown). The usefulness of the firing rate reduction at the single neuron level encourages the extension of this approach to networks of synaptically interacting IFB neurons. This is the subject of the next section.
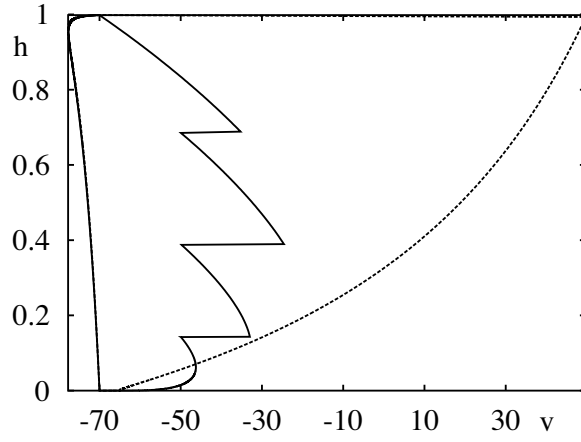
8

FIG. 2: Phase space trajectories of periodic solutions in the spiking and rate IFB model. Parameters as in Fig. 1.

III.   DISCRETE NETWORKS

Consider a network of IFB neurons with state variables (v_i, h_i), $i = 1, \ldots, N$ and synaptic conductances of the form

$$u_i(t) = g \sum_j w_{ij} \sum_m \eta(t - \sigma_m^j). \tag{10}$$

Here $u_i(t)$ represents the shape of the train of postsynaptic conductance changes induced at neuron i, by the arrival of action potentials from other neurons. The mth firing time of the jth neuron is given by σ_m^j. The parameters w_{ij} may be used to specify appropriate neuronal architectures, whilst $g > 0$ is some overall scale parameter for synaptic interaction strength. For clarity we shall focus on the case that the function $\eta(t)$ describes a so-called alpha function with $\eta(t) = \alpha^2 t \exp(-\alpha t)$ and $\eta(t) = 0$ for $t \leq 0$. Particularly for simulation purposes it is convenient to write u_i as the solution to

$$\frac{1}{\alpha} \dot{u}_i = y_i - u_i$$
$$\frac{1}{\alpha} \dot{y}_i = -y_i, \tag{11}$$

with y_i discontinuously updated according to $y_i \rightarrow y_i + g w_{ij} \alpha$ at times σ_m^j. To obtain a firing-rate model we consider the limit of slow synapses, where α^{-1} is large compared to other natural time scales of the network, so that the input to each neuron, $I_i(t) = u_i(t)(v_i - v_u)$,

9

varies slowly compared to all the v_i. A reduction of (10) is naturally obtained after writing it in the form

$$u_i(t) = g \sum_j w_{ij} \int_0^\infty \eta(s) \sum_m \delta(s - t + \sigma_m^j) \mathrm{d}s. \tag{12}$$

We then replace the spike train in (12) with some smooth function of the steady state voltage value of neuron j. The natural choice for this function is the firing rate function given by (6). The firing rate model is then completely specified by the dynamics for h_i, given by (2), the steady state voltage $v(h_i, u_i)$ given by (5) for each neuron, and the synaptic input with

$$u_i(t) = g \sum_j w_{ij} \int_0^\infty \eta(s) f(v_j(t - s)) \mathrm{d}s, \tag{13}$$

or equivalently

$$\frac{1}{\alpha} \dot{u}_i = y_i - u_i$$
$$\frac{1}{\alpha} \dot{y}_i = g \sum_j w_{ij} f(v_j) - y_i. \tag{14}$$

Although it is possible to analyze the dynamics of the full spiking model explicitly using the techniques in [14], the firing rate model is much preferred. It is continuous in time and does not require precise knowledge about spike timing.

To illustrate the usefulness of the firing rate reduction for synaptic interactions we consider a concrete problem in rhythmogenesis, namely the generation of an alternating rhythm in a network with reciprocal inhibitory synaptic coupling. We shall take as our model a *half-center oscillator* two neuron TC IFB network, where each of the identical neurons in isolation is non-oscillatory. The neuronal architecture is specified by $w_{ij} = 1 - \delta_{ij}$. For an appropriate choice of g and v_u the rebound current can be activated leading to a burst of activity. This burst causes a sequence of inhibitory post synaptic potentials (IPSPs) in the partner neuron driving it below v_h and leading to an increase in the value of its associated rebound variable, h. Upon *release* from inhibition, when the total IPSP has decayed, the partner neuron crosses the bursting threshold v_h from below and will generate a burst of its own if its rebound variable is sufficiently large. The process may then repeat ad infinitum. An example of such a rhythm is shown in Fig. 3. In Fig. 4 we show a plot of the rhythm in the (v, h) plane. The corresponding simulations of the firing rate model show similar patterns of activity, especially for small C.
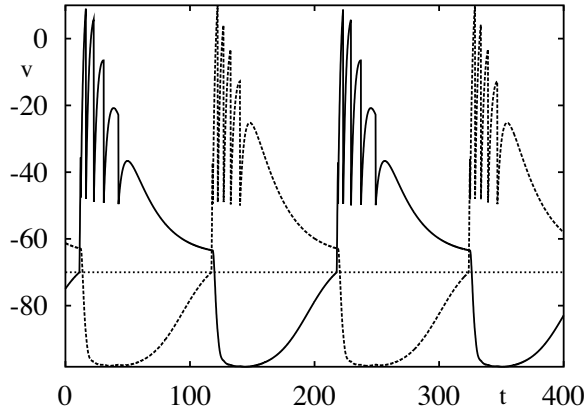
FIG. 3: A half-center oscillation in a network of two reciprocal inhibitory TC IFB cells. Parameters are $\alpha = 0.1$, $g = 5$, $v_u = -100$ and $C = 0.2$.
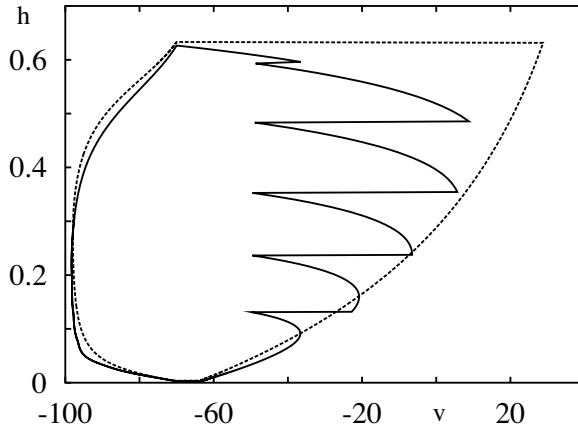

FIG. 4: Periodic orbit in (v, h) phase plane for the IFB spike and rate half-center oscillator. Parameters as in Fig. 3.

In the firing rate framework the form of the half center solution is given by $v_1(t) = v(t) = v_2(t - \Delta/2)$, where $v(t)$ is defined on $[0, \Delta)$ and is periodically extended outside this domain. The period Δ can be determined from the time spent above and below v_h, which we denote as $\Delta^{\pm}$ respectively. The simultaneous solution of $v(\Delta) = v_h$ and $v(\Delta^+) = v_h$ then determines $\Delta = \Delta^+ + \Delta^-$. For convenience we choose an origin of time such that at $t = 0$ v_1 crosses v_h from below. For a general firing rate function it is hard problem to calculate $\Delta^{\pm}$. However, we note that the model is relatively insensitive to the detailed shape of f (since interspike intervals are largely governed by the refractory process) and rather the time that
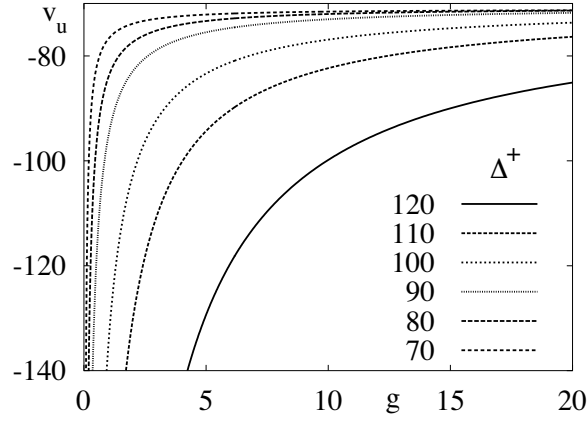
11

FIG. 5: Contour plot of solutions with fixed Δ^+ in the (g, v_u) parameter plane for the firing rate half-center oscillator. Parameters as in Fig. 3.

v spends above or below v_θ, which we denote Δ_θ. To make analytic progress we consider the replacement $f(v) \to \tau_R^{-1}\Theta(v - v_\theta)$, expected to hold in the limit $C \to 0$. Assuming that $\Delta/2 > \Delta_\theta$ and that only the most recent burst is influential the variable $u_1 \equiv u$ may be written

$$u(t) = \frac{g}{\tau_R}Q(t - \Delta/2, \min(\Delta_\theta, t - \Delta/2)), \qquad t \in [\Delta/2, 3\Delta/2) \tag{15}$$

where

$$Q(t, a) = \int_0^a \eta(t - s)\mathrm{d}s. \tag{16}$$

Note that outside its natural domain we periodically extend $u(t)$. For an α function we have that

$$Q(t, a) = \mathrm{e}^{-\alpha(t-a)}[1 + \alpha(t - a)] - \mathrm{e}^{-\alpha t}[1 + \alpha t]. \tag{17}$$

The three unknowns $\Delta, \Delta^+, \Delta_\theta$ may then be found by the simultaneous solution of the three equations $v(\Delta_\theta) = v_\theta$, $v(\Delta^+) = v_h$ and $v(\Delta) = v_h$ ($\Delta > \Delta^+$). Here, $v(t) = v(h(t), u(t))$ from (7), with u given by (15), h by (8) and $s = 1$ for $t \in [0, \Delta^+]$ and is zero otherwise. The numerical solution of this system of equations may be used to calculate the parameter sets for half-center oscillations of a given period or given burst duration. In Fig. 5 we present the results of such a calculation giving the locus of points in the (g, v_u) parameter plane where half-center oscillations have a fixed Δ^+. This figure shows that the time spent above v_h can be increased by either decreasing v_u or increasing g, both of which describe an increased level of mutual inhibition. The techniques that we have described above are also ideally suited
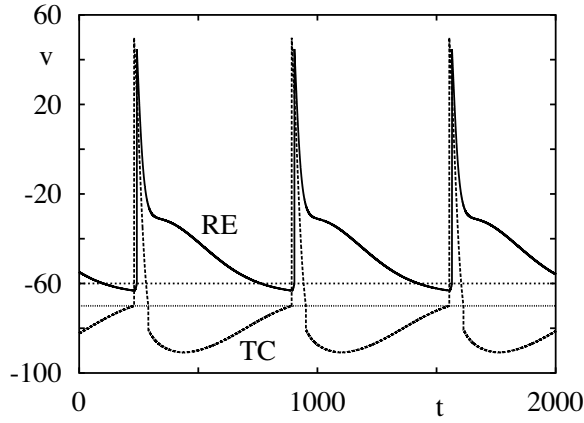
12

FIG. 6: Dynamics of an RE-TC pair within the firing rate formalism. Parameter values are $g = 2$, $\alpha = 0.01$, $v_{\text{GABA}} = -100$ and $v_{\text{AMPA}} = 0$. For simplicity we have assumed that the time course and strength of AMPA and GABA$_\text{A}$ synapses is the same.

to studying mixed networks of both RE and TC IFB neurons. In particular it allows us to examine one of the basic circuits found in thalamus, namely an RE-TC pair. For a recent overview of the behavior of this and more extensive thalamocortical circuits we refer the reader to the book by Destexhe and Sejnowski [6]. It is worth briefly considering a reciprocal RE-TC circuit where the inhibitory synapse onto the TC cell is GABA$_\text{A}$ mediated and the excitatory one onto the RE cell AMPA mediated. This sets the scene for the discussion of large networks that will be presented in the next section. Rather than use labels $i = 1, 2$ we shall simply use subscript (RE) and (TC) to distinguish between the two cell types and denote the corresponding synaptic reversal potentials as v_{AMPA} and v_{GABA} respectively. An example of the type of rhythm that can be generated by this RE-TC network is shown in Fig. 6. We summarize the behavior of the oscillating system as follows. The TC cell fires upon release from inhibition. There is then a sudden build up of activity in the RE cell, which fires a burst of spikes. Eventually the spike packet generated by the RE cell terminates as h_{RE} decays back to zero. During this period the TC cell is inhibited. The intrinsic dynamics of the RE cell is such that v_h is crossed from above and h_{RE} increases towards one ready to release another barrage of spikes upon receiving excitatory input, caused by release of inhibition of the TC cell. This process is free to repeat over, leading to the generation of a periodic oscillation. A basic observation that we wish to make is that the natural rhythm of the circuit involves the firing of the RE cell just after the onset of firing in the TC cell.
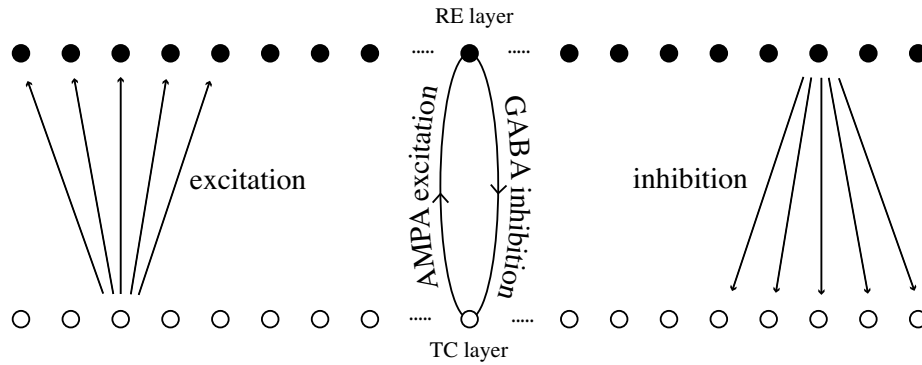
13

FIG. 7: A two layered network of TC and RE cells with reciprocal interactions. The TC cells excite the RE cells with AMPA mediated synapses. The RE cells inhibit the TC cells with GABA_A mediated synapses.

Hence, in some sense the circuit can generate a nearly synchronous activity between an RE and TC cell. We shall use this observation in the next section to consider the reduction of two-layer reciprocally interacting networks of RE and TC cells to single layers of either purely RE cells or purely TC cells.

IV. CONTINUOUS NETWORKS

A number of continuum neural field models have been developed with the aim of understanding the mechanisms of pattern formation and wave propagation in spatially extended neural sheets. They are often motivated by statistical averaging over ensembles of neurons with similar functional properties, as well as temporal averaging over spike trains from individual neurons. Most of these models can trace their roots back to the work of Wilson and Cowan [17] and Amari [18] and are often written as integro-differential equations. In this section we shall consider a two-layer model of interacting RE-TC IFB cells using a neural field description. The particular network we are interested in has the same characteristics as that considered by Golomb *et al.* [7] and is depicted in Fig. 7. A continuous layer of RE cells inhibits a continuous layer of TC cells with some spreading synaptic footprint. This TC layer in turn acts back on the RE layer with a spread of excitatory connections. For

14

simplicity we ignore interactions within a layer. Motivated by previous work [7, 8, 11] we expect that a mathematical analysis of a two-layered IFB neural field model to yield solutions that describe both smooth and lurching waves. To gain insight into the dynamics of such waves, but avoiding a full mathematical treatment of a two-layered system, we focus here on a reduction to a single-layered network. Guided by the behavior of the simple RE-TC pair described in section III we consider a scenario in which the RE and TC layers are slaved together. Then on one hand we may imagine RE cells to feel an indirect spread of excitation (via the inhibitory interaction with TC cells) and on the other hand for TC cells to feel an indirect spread of inhibition (via the excitatory interaction with RE cells). In either case we have only to consider an effective single layer network that can be described with an integral equation of the form:

$$u(x,t) = g \int_{-\infty}^{\infty} w(y) \int_{0}^{\infty} \eta(s)f(v(x-y,t-s))\mathrm{d}y\mathrm{d}s. \tag{18}$$

The above equation may be regarded as the continuous space counterpart of equation (13). The effective spread of connections within the network is described with the synaptic footprint function $w(y)$. This neural field model is supplemented with the dynamics for the rebound variable $h(x,t)$ and the formula for the steady state voltage (7). For a recent discussion of the link between spiking and firing rate neural field models we refer the reader to [19]. We shall now present an analysis of waves in this model for the two cases described above; i) an excitatory RE network and ii) an inhibitory TC network.

A.   Smooth waves in RE networks

The existence and construction of smoothly propagating waves in neural field theories has been considered by several authors. In particular we refer the reader to work in [19, 20, 21, 22, 23, 24, 25]. Following the approach in these papers we consider the construction of waves in an excitatory layer of RE IFB cells. Within the firing rate framework we consider solutions of the form $f \circ v(x,t) = f \circ v(t-x/c)\Theta(t-x/c)$, where we identify c with a wave speed. If we adopt a traveling wave frame where $\xi = ct - x$ then $u(x,t) = u(\xi)$ and we may write

$$u(\xi) = g \int_{0}^{\infty} w(\xi'-\xi)E(\xi'/c)\mathrm{d}\xi', \tag{19}$$
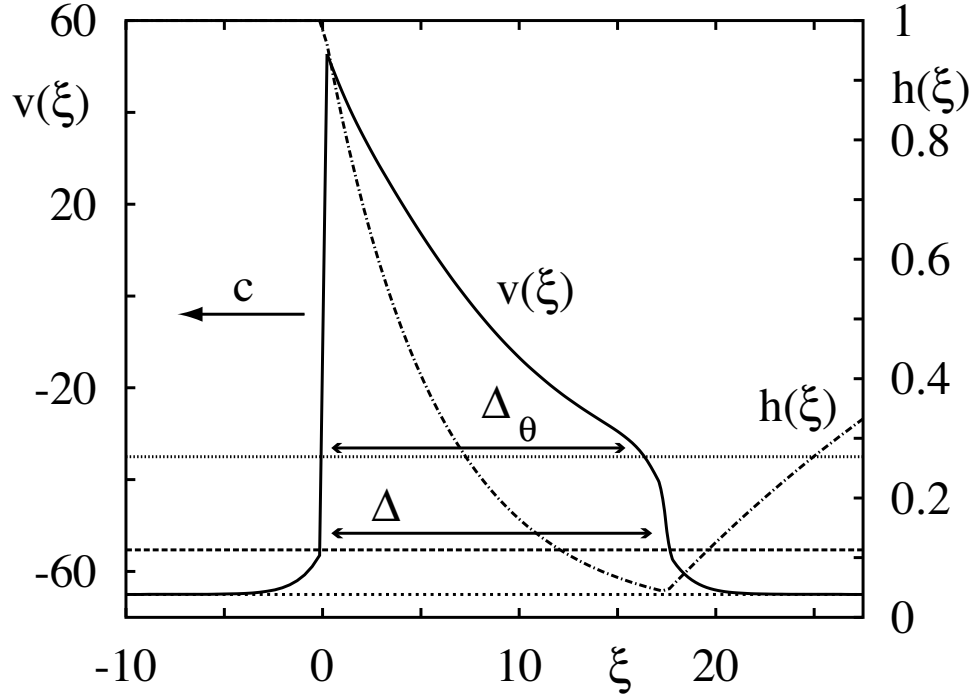
FIG. 8: An example of a solitary wave in an RE network with excitatory synaptic feedback, obtained as an exact solution to the Heaviside firing rate equations. Here, $v_h = -55$, $\alpha = 1.0$, $g = 0.1$, $v_u = 0$ and $\sigma = 1$.

where

$$E(\xi) = \int_0^\xi \eta(\xi - s) f \circ v(s) \mathrm{d}s. \tag{20}$$

We shall now consider the construction of a solitary pulse solution for the case that the firing rate function is a Heaviside. We denote the duration of firing by Δ_θ, the time that h is deinactivated by Δ and choose an origin in the traveling wave frame at the point where the system first starts firing. An illustration of such a solution is given in Fig. 8. In this case we have simply that $E(\xi) = Q(\xi, \min(\Delta_\theta, \xi))/\tau_R$, with Q given by (16). For the choice

$$w(x) = \frac{1}{2\sigma} \exp(-|x|/\sigma), \tag{21}$$

the solution (19) may be expressed in closed form, by evaluating some appropriate integrals. The details of this calculation are presented in the appendix. Exploiting the piecewise linear

16

nature of the rebound dynamics shows that the dynamics for h has a simple form given by

$$h(\xi) = \begin{cases} 1 & \xi \leq 0 \\ e^{-\xi/c\tau_h^-} & 0 < \xi < \Delta \\ 1 - (1 - \overline{h})e^{-(\xi-\Delta)/c\tau_h^+} & \xi \geq \Delta \end{cases} \qquad (22)$$

where $\overline{h} = \exp(-\Delta/c\tau_h^-)$. The speed of the traveling pulse is defined by the three conditions $v(0) = v_h$, $v(\Delta_\theta) = v_\theta$ and $v(\Delta) = v_h$. Numerical solution of these three equations shows that the speed of a solitary wave in an excitatory RE network is relatively insensitive to the choice of g or σ. However, as expected, there is a strong dependence on v_h. In Fig. 9 we plot $c = c(v_h)$, showing the wave speed c as a function of v_h. With increasing v_h a fast and slow branch are seen to annihilate leading to propagation failure of the solitary pulse. As v_h approaches v_L from above one sees waves of increasing speed. Direct numerical simulations of a network in MATLAB show excellent agreement with the theoretical predictions and are plotted as crosses in Fig. 9. Moreover, these simulations show that it is the faster of the two branches that is stable.

We note that under the replacement $f \circ v(\xi) = \delta(\xi)$, valid in the extreme limit $\Delta_\theta \to \tau_R \to 0$, then equation (19) becomes equivalent to the input considered by many other authors within the context of spiking IF [9, 10, 26, 27, 28, 29] and theta neuron networks [30, 31, 32]. The speed of the wave is then simply determined by $u(0) = v_h$, which is the type of condition that occurs in the theory of traveling pulses (single spike) for IF networks. In this case Bressloff [28, 29] and Golomb and Ermentrout [9, 10] have already shown that it is the fast wave that is stable. However, with the inclusion of discrete delays, $\eta(t) \to \eta(t - \tau_d)$, a fast pulse can destabilize in favor of a lurching pulse. In the next section we show how lurching waves may originate in an inhibitory TC network without discrete delays.

B. Lurching waves in TC networks

When neurons can fire via post inhibitory rebound it is well known that this can lead to lurching waves of activity propagating through an inhibitory network [8]. A lurching wave does not travel with a constant profile, (i.e., there is no traveling wave frame) although it is possible to identify a lurching speed. Rather, the propagating wave recruits groups of cells in discrete steps. The leading edge of active cells inhibits some cluster of cells
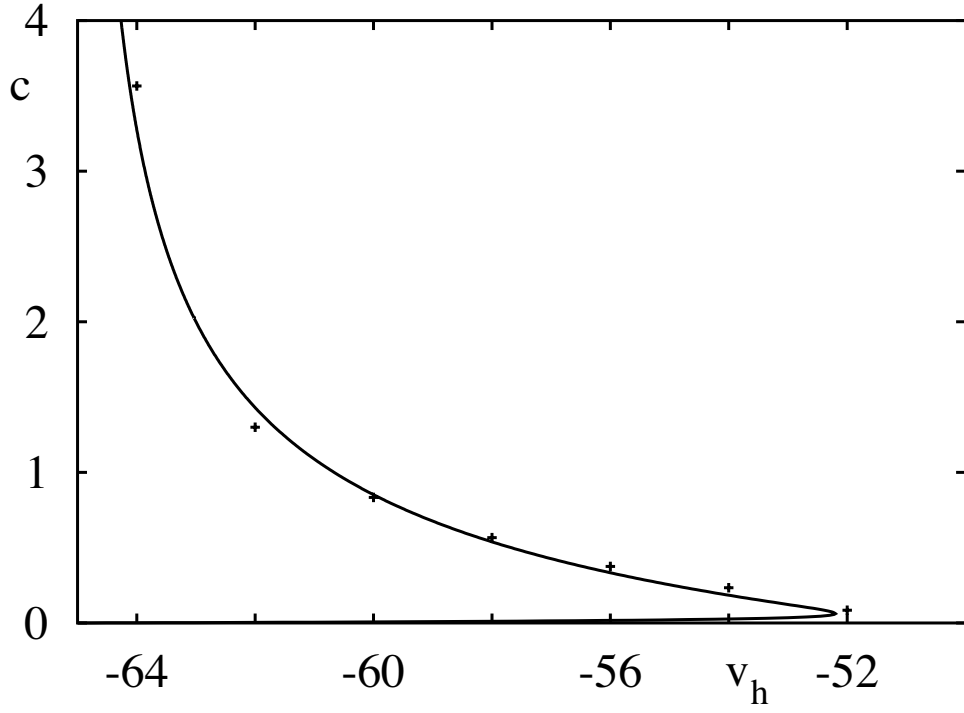
17

FIG. 9: Speed of a solitary pulse in an excitatory RE network. Parameters as in Fig. 8. Crosses denote the results of numerical simulations in MATLAB done on a network of size 50σ using a mesh of 2^8 grid points. In all simulations the synaptic inputs are computed using the MATLAB `conv` function and all equations are evolved forward in time using `ODE45`. The steady state value of voltage $v = v(h, u)$ is obtained by numerically evolving (1) with very small C, so that compared to the dynamics for u, v is a *fast* variable.

ahead of it (depending on the size of the synaptic footprint). Inhibited cells (ahead of the wave) must wait until they are released from inhibition before they can, in turn, fire. The mathematical analysis of such non-smooth waves has been undertaken by Terman *et al.* using the techniques of geometric singular perturbation theory [11]. For models that arise as reduced models for thalamic neurons these authors have been able to construct very good estimates for various properties of lurching pulses, such as the time between successive release events. In this section we show how an exact analysis of lurching waves can be performed for a minimal thalamic network built out of inhibitory IFB TC cells. In common with other more complicated models of thalamic neurons, IFB TC neurons have the ability to fire via post inhibitory rebound. For mathematical convenience we work with the Heaviside firing

FIG. 10: A diagram of an idealized solitary lurching pulse showing the four unknowns that parameterize the solution. Here L represents the size of a cluster, T_L the period of the lurch, Δ_θ the time spent firing and Δ the duration of inhibition where the rebound variable h is increasing. Grey regions indicate where the system is firing.

rate function and consider

$$w(x) = \frac{1}{2\sigma}\Theta(\sigma - |x|). \tag{23}$$

We denote the size of a cluster involved in a lurch by L. For simplicity we shall only consider lurching pulses where consecutive active clusters are adjacent to each other. We suppose that to a first approximation neurons for $x \in (0, L)$ are simultaneously released from inhibition and start firing at time $t = T_L$. The next group with $x \in (L, 2L)$ fires when $t = 2T_L$. We define the firing duration of a cluster as Δ_θ (i.e., the time spent above v_θ) and the duration of inhibition (time spent below v_h before release) as Δ. An illustration of this type of lurching pulse is shown in Fig. 10. Assuming that the system starts at rest with $h(x, 0) = 0$, then $h(x, T_L) = 1 - \exp(-\Delta/\tau_h^+) \equiv \overline{h}$ for $x \in (0, L)$. Hence, for $t > T_L$,

$$h(x, t) = \overline{h}e^{-(t-T_L)/\tau_h^-}, \qquad x \in (0, L). \tag{24}$$

To calculate the synaptic conductance (18) we assume that for $x \in (0, L)$ and $t > 0$ the dominant contribution arises from the activity on $x \in (-L, 0)$ for $t \in (0, \Delta_\theta)$. The expression for (18) then takes the simple (separable) form

$$u(x, t) = \frac{g}{\tau_R} Q(t, \min(t, \Delta_\theta)) W(x), \qquad x \in (0, L), \ t > 0, \tag{25}$$

where

$$W(x) = \int_x^{x+L} w(y) \mathrm{d}y = \begin{cases} L/2\sigma & x + L < \sigma \\ (\sigma - x)/2\sigma & x + L > \sigma \end{cases}. \tag{26}$$

Hence, using (7), we have a closed form expression for $v(x, t)$ in terms of the four unknowns L, T_L, Δ and Δ_θ. Note that if $2L < \sigma$ then $W(x) = L/2\sigma$ and $u(x, t)$ given by (25) is independent of x. Assume to a first approximation that $v(x, t) = v(0, t)$ for $x \in (0, L)$, then three of the unknowns are determined by the simultaneous solution of $v(0, T_L) = v_h$, $v(0, T_L + \Delta_\theta) = v_\theta$ and $v(0, T_L - \Delta) = v_h$. The first condition determines the time of release from inhibition, the second determines the firing duration and the third determines the time of onset of inhibition. To obtain a final constraint we note that the assumption of simultaneous firing within a cluster is not strictly true (unless $L < \sigma/2$) and that $v(x, t) \neq v(0, t)$ for $L > \sigma/2$ (which can be seen from (25) and (26)). We define the size of a cluster using the constraint $v(L, T_L) = v_h$. Since $W(L)$ takes its maximal value for $L = \sigma/2$ we see that there is a solution with $L = \sigma/2$. A numerical solution of these four simultaneous equations is presented in Fig. 11. Lurching waves are found for $v_h < v_L$, with $T_L \to \infty$ as $v_h \to v_L$. Moreover, T_L decreases with decreasing v_h and a solution is lost in a saddle-node bifurcation. Direct numerical simulations performed in MATLAB show excellent agreement with the theory. Note that as in the work of Terman *et al.* we set self-inhibition to be zero in simulations to better see the emergence of lurching waves from initial data (which we take to be in the form of a localized depolarization of the system at one end). Note that in their analysis Terman *et al.* partly rely on data from numerical solutions to construct lurching speed estimates and hence can not obtain unstable solution branches like we have managed here. If we introduce a lurch velocity $v = L/T_L$ we see from Fig. 11 that in contrast to waves in RE systems it is the slow wave which is stable. In Fig. 12 we illustrate that T_L increases with g, which is also consistent with the results of Terman *et al.*
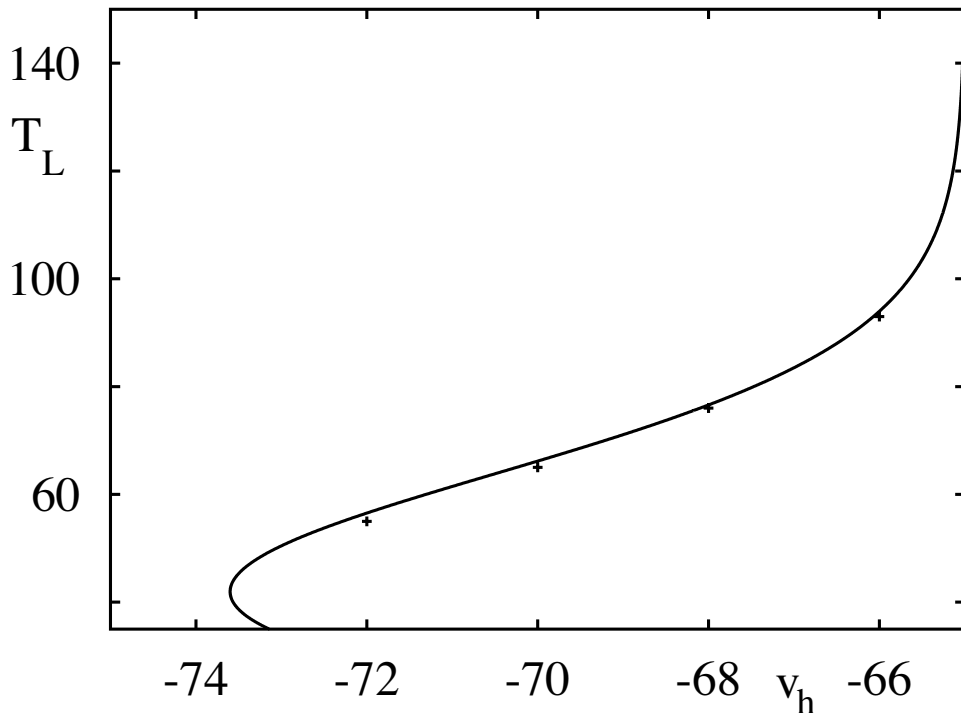
FIG. 11: Period of a solitary lurching pulse in an inhibitory TC network as a function of v_h. Parameters as in Fig. 8, but with $\alpha = 0.1$, $g = 1.0$ and $v_u = -100$. Crosses denote the results of numerical simulations done on a network of size $N\sigma/2$ using a mesh of $N = 2^8$ grid points.

V. DISCUSSION

In this paper we have presented a firing rate reduction of the IFB neuron model. When the firing rate output of the neuron is dominated by a refractory process we have shown that the model can be exactly solved for a number of important cases. We have illustrated this by considering simple central pattern generating networks of synaptically interacting IFB neurons. Direct numerical simulations have shown that, for slow synapses, there is good agreement between spiking and firing rate IFB networks. In light of the ability of IFB neurons to replicate the dynamics of both TC and RE cells this opens up the way for a mathematical study of thalamic circuits. One step in this direction has been presented here, with a study of traveling waves in continuous firing rate networks of IFB neurons. We have been able to construct a smooth fast traveling pulse in a network of excitatory RE cells and a slow lurching pulse in a network of inhibitory TC cells. Our results are consistent with previous studies of more detailed models of neural networks with slow T-type calcium
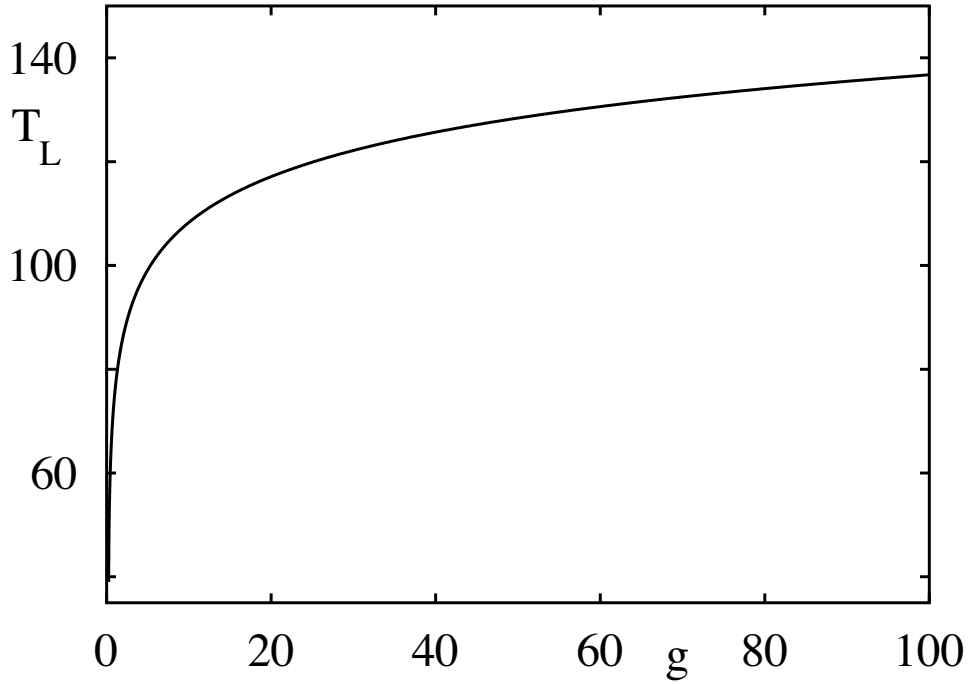
21

FIG. 12: Period of a solitary lurching pulse in an inhibitory TC network as a function of the strength of conductance. Parameters as in Fig. 11 with $v_h = -70$.

currents. Importantly, the mathematical tractability of our model network will allow a number of further studies.

Although, for clarity of exposition, we have focused on single layer networks, the techniques we have described generalize naturally to multi-layer structures. Indeed a more complete study of a truly two-layered RE-TC network may shed light on the properties of mixed-wave solutions where, for example, a lurching front may leave behind a periodic wave in its wake. The study of two-layered networks is also of interest from a sensory processing point of view. It is well known that sensory thalamic nuclei can act as a state-dependent *gateway* between the sensory periphery and higher cortical centers [33]. A two-layered RE-TC IFB firing rate network can be used as testing ground for the effects of synaptic footprint shapes on network filtering properties. In particular the simplicity of the model should allow for the calculation of network response to a spatio-temporal pattern. For example, within the context of the visual system one could consider retiongeniculate input to TC cells by convolving an experimentally relevant illumination profile (such as a drifting grating) with the spatio-temporal receptive field of a retinal ganglion cell. This may allow one to go be-

yond the traditional linear response analysis of geniculate circuits [34]. The work in this paper also raises the interesting mathematical question of wave stability. There has been some recent progress on the asymptotic stability of traveling waves in integro-differential equations that, when generalized to include rebound currents, may answer the question for the smooth waves seen in excitatory RE networks [23, 35]. However, the stability of lurching waves is likely to require the development of new analytical techniques to handle the fact that it is not possible to move to a co-moving frame. These and related issues are all topics of current investigation.

Acknowledgements

Appendix

The traveling pulse in an excitatory RE network may be constructed from (19) using the result that $E(\xi) = Q(\xi, \min(\Delta_\theta, \xi))/\tau_R$ (valid when the firing rate function is a Heaviside, i.e., $f \circ v(\xi) = \Theta(\xi)\Theta(\Delta_\theta - \xi)/\tau_R$). Consider first the case that $\xi < 0$. Using (21) we have that

$$
\begin{aligned}
u(\xi) &= \frac{g}{2\sigma\tau_R} \int_0^\infty e^{-(\xi'-\xi)/\sigma} Q(\xi'/c, \min(\xi', \Delta_\theta)/c)\mathrm{d}\xi' \\
&= \frac{g e^{\xi/\sigma}}{2\sigma\tau_R} \left\{ \int_0^{\Delta_\theta} e^{-\xi'/\sigma} Q(\xi'/c, \xi'/c)\mathrm{d}\xi' + \int_{\Delta_\theta}^\infty e^{-\xi'/\sigma} Q(\xi'/c, \Delta_\theta/c)\mathrm{d}\xi' \right\}.
\end{aligned}
\tag{27}
$$

By writing equation (17) in the form

$$
Q(t, a) = \widetilde{Q}(t - a) - \widetilde{Q}(t),
\tag{28}
$$

where

$$
\widetilde{Q}(t) = \left[1 - \alpha\frac{\mathrm{d}}{\mathrm{d}\alpha} \right] e^{-\alpha t},
\tag{29}
$$

it is then relatively straightforworward to evaluate the integrals in (27). These may be expressed in terms of the function $W(a, b)$ and $G_\pm(a, b, d)$ where

$$
W(a, b) = \int_a^b e^{-\xi'/\sigma}\mathrm{d}\xi' = \sigma[e^{-a/\sigma} - e^{-b/\sigma}],
\tag{30}
$$

23

and

$$G_\pm(a, b, d) = \int_a^b e^{-\xi'/\sigma} \widetilde{Q}((\pm\xi' - d)/c) d\xi'$$

$$= \gamma_\pm \left\{ e^{-a/\sigma} e^{\alpha(d\mp a)/c}[1 - \alpha(d \mp a)/c \pm \gamma_\pm/c] \right.$$

$$\left. - e^{-b/\sigma} e^{\alpha(d\mp b)/c}[1 - \alpha(d \mp b)/c \pm \gamma_\pm/c] \right\}. \tag{31}$$

Here

$$\frac{1}{\gamma_\pm} = \frac{1}{\sigma} \pm \frac{\alpha}{c}. \tag{32}$$

Equation (27) then takes the form $u(\xi) = g e^{\xi/\sigma} \phi_1/2\sigma\tau_R$ with ϕ_1 given by

$$\phi_1 = W(0, \Delta_\theta) - G_+(0, \Delta_\theta, 0) + G_+(\Delta_\theta, \infty, \Delta_\theta) - G_+(\Delta_\theta, \infty, 0). \tag{33}$$

In a similar fashion it may be shown that $u(\xi) = g\phi_2(\xi)/2\sigma\tau_R$ for $0 \leq \xi \leq \Delta_\theta$ with

$$\phi_2(\xi) = W(0, \xi) - G_-(0, \xi, -\xi) + W(0, \Delta_\theta - \xi) - G_+(0, \Delta_\theta - \xi, -\xi)$$

$$+ G_+(\Delta_\theta - \xi, \infty, \Delta_\theta - \xi) - G_+(\Delta_\theta - \xi, \infty, -\xi), \tag{34}$$

and $u(\xi) = g\phi_3(\xi)/2\sigma\tau_R$ for $\xi > \Delta_\theta$, where

$$\phi_3(\xi) = G_-(0, \xi - \Delta_\theta, \Delta_\theta - \xi) - G_-(0, \xi - \Delta_\theta, -\xi) + W(\xi - \Delta_\theta, \xi) - G_-(\xi - \Delta_\theta, \xi, -\xi)$$

$$+ G_+(0, \infty, \Delta_\theta - \xi) - G_+(0, \infty, -\xi). \tag{35}$$

---

[1] M. Steriade, E. G. Jones, and R. R. Línas, *Thalamic Oscillations and Signalling* (Wiley, New York, 1990).

[2] M. von Krosigk, T. Bal, and D. A. McCormick, Science **261**, 361 (1993).

[3] T. Bal, M. von Krosigk, and D. McCormick, Journal of Physiology (London) **483**, 641 (1995).

[4] T. Bal, M. von Krosigk, and D. McCormick, Journal of Physiology (London) **483**, 665 (1995).

[5] U. Kim, T. Bal, and D. A. McCormick, Journal of Neurophysiology **84**, 1301 (1995).

[6] A. Destexhe and T. Sejnowski, *Thalamocortical Assemblies* (Oxford University Press, 2001).

[7] D. Golomb, X.-J. Wang, and J. Rinzel, Journal of Neurophysiology **75**, 750 (1996).

[8] J. Rinzel, D. Terman, X. J. Wang, and B. Ermentrout, Science **279**, 1351 (1998).

[9] D. Golomb and B. Ermentrout, Proceedings of the National Academy of Sciences USA **96**, 13480 (1999).

[10] D. Golomb and G. B. Ermentrout, Network **11**, 221 (2000).

[11] D. H. Terman, G. B. Ermentrout, and A. C. Yew, SIAM Journal on Applied Mathematics **61**, 1578 (2001).

[12] G. D. Smith, C. L. Cox, S. M. Sherman, and J. Rinzel, Journal of Neurophysiology **83**, 588 (2000).

[13] G. D. Smith and S. M. Sherman, Journal of Neuroscience **22**, 10242 (2002).

[14] S. Coombes, M. R. Owen, and G. D. Smith, Physical Review E **64**, 041914 (2001).

[15] G. D. Smith, C. L. Cox, S. M. Sherman, and J. Rinzel, Thalamus and Related Systems **11**, 1 (2001).

[16] P. C. Bressloff and S. Coombes, Neural Computation **12**, 91 (2000).

[17] H. R. Wilson and J. D. Cowan, Kybernetik **13**, 55 (1973).

[18] S. Amari, Biological Cybernetics **27**, 77 (1977).

[19] S. Coombes, G. J. Lord, and M. R. Owen, Physica D (to appear) (2003).

[20] G. B. Ermentrout and J. B. McLeod, Proceedings of the Royal Society of Edinburgh **123A**, 461 (1993).

[21] Z. Chen, B. Ermentrout, and X.-J. Wang, Journal of Computational Neuroscience **5**, 53 (1998).

[22] B. Ermentrout, Journal of Computational Neuroscience **5**, 191 (1998).

[23] L. Zhang, Ph.D. thesis, Department of Mathematics, Columbus, Ohio, USA (1999).

[24] D. J. Pinto and G. B. Ermentrout, SIAM Journal on Applied Mathematics **62**, 206 (2001).

[25] D. Terman and L. Zhang, Preprint (2002).

[26] D. Golomb and G. B. Ermentrout, Physical Review Letters **86**, 4179 (2001).

[27] D. Golomb and G. B. Ermentrout, Physical Review E **65**, 061911 (2002).

[28] P. C. Bressloff, Physical Review Letters **82**, 2979 (1999).

[29] P. C. Bressloff, Journal of Mathematical Biology **40**, 169 (2000).

[30] R. Osan and B. Ermentrout, Neurocomputing **38-40**, 789 (2001).

[31] R. Osan and B. Ermentrout, Physica D **163**, 217 (2002).

[32] R. Osan, J. Rubin, and B. Ermentrout, SIAM Journal on Applied Mathematics **62**, 1197 (2002).

[33] D. A. McCormick and T. Bal, Annual Review of Neuroscience **20**, 185 (1997).

[34] G. T. Einvoll and H. E. Plesser, Network **13**, 503 (2002).

[35] D. Terman and L. Zhang (2002), Preprint.